ALGORITHM FOR SPATIAL-SPECTRAL DATA CORRECTION CAPTURED BY A MULTISPECTRAL CAMERA

 2025 **A. A. Zolotukhina**[a,b] *, **A. S. Machikhin**[a,b], **A. V. Guryleva**[a], **G. V. Nesterov**[a], **V. V. Tedeeva**[c]

[a]*Scientific and Technological Centre of Unique Instrumentation of the Russian Academy of Sciences, Moscow, Russia*

[b]*National Research University «Moscow Power Engineering Institute», Moscow, Russia*

[c]*The North Caucasian Research Institute of Mountain and Piedmont Agriculture – the Affiliate of Vladikavkaz Scientific Centre of the Russian Academy of Sciences, Mikhailovskoye, Russia*

**e-mail: zolotukhina.aa@ntcup.ru*

Received November 14, 2024

Revised December 03, 2024

Accepted December 30, 2024

Abstract. Imaging spectrometers provide non-contact and high-performance assessment of the physical and chemical object properties distribution, the effectiveness of which depends on the data accuracy obtained by the device. The paper introduces a method to correct spatial-spectral distortions in images captured by the imaging spectrometer based on the optical aperture division.

Keywords: *spectral imaging, multispectral camera, calibration, distortion correction, digital image processing*

DOI: 10.31857/S03676765250419e2

INTRODUCTION

Multispectral cameras or video spectrometers with multispectral resolution are in demand for solving problems in agriculture, environmental monitoring, biomedical and technical diagnostics [1]. The most reliable and productive measurement of spectral and spatial characteristics of objects from moving carriers [2] or analysis of fast processes [3] is guaranteed by devices with simultaneous registration of several spectral images of objects. To perform measurements on the basis of such data, it is necessary to determine the parameters for correction of their distortions introduced by the hardware and imaging conditions, and to carry out further calibration of the instrument to unify its characteristics [4,5].

Due to the variety of physical principles of spatial-spectral data acquisition [6], there is no single unified method for calibrating video spectrometers and correcting the data recorded with them. Calibration and correction methods developed for a device based on a certain registration scheme [7,8] are inapplicable and ineffective for data correction of a device built on a different principle. Earlier the authors proposed a new principle of multispectral imaging based on optical aperture separation [9], which favorably differs from its analogues by a set of key features (number of spectral channels, performance, reliability, adaptability to a specific task, etc.). The purpose of this work is to develop an algorithm for multispectral camera calibration based on optical aperture separation and correction of the data recorded by it.

FORMATION OF SPECTRAL IMAGES BY A MULTISPECTRAL CAMERA

The multispectral camera based on optical aperture separation, developed at the RAS UE STC, includes a multispectral module and a matrix radiation receiver. The main elements of the multispectral module are optical systems of spectral image formation (spectral channels), each of which consists of a lens and a spectral filter. Such optical systems are installed in a single body of the multispectral module in front of the matrix radiation receiver and simultaneously form several spatially separated spectral images on it. Fig. 1 shows a block diagram of spectral images formation in a multispectral camera built according to the above scheme.

Spectral imaging is usually aimed at determining the spatial and spectral distribution of the ability of the object under study to reflect the incident radiation, i.e. at determining the reflection coefficient ρ (x, y, λ). The data obtained with the multispectral camera represent the intensity distribution of the radiation reflected from the observed object and passed through the optical system along two spatial (x, y) and one spectral (λ) coordinates. The registered spatial-spectral intensity distribution is distorted by each functional block of the instrument and also depends on the imaging conditions, primarily on the nature of object illumination. The main sources of data distortion are shown in Fig. 1.

The intensity of radiation reflected from an object is determined by both ρ (x, y, λ) and the illumination distribution on its surface created by the radiation source. The illuminance E (x, y, λ) can have both spatial and spectral heterogeneity, and thus introduce distortions into the computed distribution ρ (x, y, λ). The radiation reflected from the object passes through the optical system, whose main distortions in the 16-channel multispectral camera implementation [10] are due to the presence of distortion D (x', y', λ) and vignetting V (x', y', λ) in the lenses. These system properties are present due to the wide field of view of the lenses and reduce the fidelity of the features more at the edges of the field of view. In addition, spectral filters can also have spectral τ (λ) and spatial τ (x', y') inhomogeneity of the transmission function, while unique for each channel.

The use of independent spectral channels with a field of view offset can lead to the appearance of parallax, which is especially noticeable in systems with multiple receivers, but has less effect in the considered system with optical aperture separation. The receiver in the camera converts the optical radiation incident on it into discrete intensity values at the ADC output, which are affected by digital noise of various nature $I_W(x', y', \lambda)$. In addition, the signal is distorted due to spatial and spectral non-uniformity of the detector sensitivity S (x', y', λ), which leads to distortions of spectral characteristics of objects .

ALGORITHM FOR CORRECTION AND CALIBRATION OF MULTISPECTRAL DATA

The purpose of correction of the data recorded by the device is to calculate the actual distribution of the object surface reflectance ρ (x, y, λ) based on the signal I (x', y', λ) recorded by the camera in each channel. During the correction, the instrument is calibrated using standard objects with known characteristics [11] to determine the parameters of distortion compensation. As a rule, these parameters are correction coefficients that change the intensity of pixels of the registered frames, as well as the magnitudes and directions of vectors for their local and global shifts. Then the obtained parameters are applied to real data to eliminate spatial-spectral artifacts arising during their registration by software means.

The signal recorded by the multispectral camera includes both the useful signal ρ (x, y, λ) and its distorting components of different nature. Elimination of each of such components requires a separate calibration procedure and subsequent distortion compensation. Fig. 2 shows the main steps of the proposed algorithm for multispectral camera data correction based on optical aperture division.

Correction of noise of radiation receiver components can be made by subtraction from the corrected frames of images obtained in the absence of radiation falling on the matrix receiver. In this case it is necessary to set the same values of exposure time and amplification as were set when capturing the corrected spectral images.

We propose to correct vignetting using the method of correction factors described in [11]. For this purpose we registered spectral images of the output window of the integrating sphere LabSphere FT-2200-W, which provides spatially and spectrally uniform radiation when its intensity changes with some step. Averaging of pixel intensities of the obtained images and normalization of the obtained image to the maximum value allows us to obtain a matrix of correction factors for each spectral channel.

Coefficients for distortion correction in each channel of the multispectral module were obtained using spectral images of the checkerboard world using the algorithm described in [12]. Then, to eliminate the influence of parallax and to match spectral images in separate channels, the shift vectors for each channel were determined relative to the reference channel from the registered crosshair images.

Various radiometric calibration methods can be used to calculate the spatial distribution of the spectral reflectance [13]. In this work, an empirical method was chosen that allows radiometric calibration to be performed both in the laboratory and in the field.

APPROBATION OF THE ALGORITHM IN LABORATORY AND FIELD CONDITIONS

In order to evaluate the effectiveness of the proposed correction algorithm, we determined the calculation error of the spectral characteristics of the color target. Beforehand, we measured the spectral reflection coefficients of each region of the color target using the spectrophotometer SF-2000. In Fig. 3 shows the spectral reflectance measured by the spectrophotometer (solid line) and calculated from the multispectral camera data after correction (dashed line). The spectrum-averaged relative error of $\rho(x, y, \lambda)$ determination from the corrected data was 5%, while without applying the camera distortion correction algorithm, the error of reflectance determination after radiometric calibration is 38%.

Since one of the main applications of multispectral cameras is monitoring the physiological state of vegetation, the proposed algorithm of spatial-spectral data correction was applied to spectral images of crops. For this purpose, 7 soybean varieties were imaged on the territory of the experimental field of the North Caucasus Research Institute of mountain and foothill agriculture of the All-Russian Scientific Center of the Russian Academy of Sciences. Using multispectral imaging data according to the method described in [14], we obtained the spatial distribution of the content of total chlorophyll in leaves (Fig. 4), which is one of the most demanded for assessing the efficiency of photosynthesis in the tasks of optimization of agrotechnical operations and phytosanitary monitoring [15]. Further, the values of total chlorophyll concentrations obtained by chemical laboratory analysis and by multispectral imaging data before and after correction were compared. The comparison showed that data correction allowed to reduce the error in determining total chlorophyll concentrations from multispectral imaging data from 47% to 10%.

CONCLUSION

Thus, we have proposed a method of video spectrometer data correction based on optical aperture separation. The developed approach makes it possible to obtain the distribution of the spectral reflectance of the object without distortions caused by spatial and spectral inhomogeneities of the device and illumination characteristics. The algorithm provides a reduction of the average relative error in determining the spectral characteristics of the object from 38 to 5%. The obtained results contribute to the introduction of a new method of multispectral imaging for solving actual problems of agriculture, environmental monitoring and medical diagnostics.

In terms of the development of the field experiment scheme and sample preparation, the publication was prepared within the framework of the state assignment of the All-Russian Scientific Center of RAS No. 075-01005-23-00. In terms of development of methods for calibration of the instrument and correction of the data recorded by it. The work was carried out within the framework of the state assignment of RAS STC UP (project FFNS-2022-0010).

FUNDING

The results of the work were obtained using the equipment of the Center for Collective Use of the Scientific and Technological Center for Unique Instrumentation of the Russian Academy of Sciences (STC UP RAS) (https://ckp.ntcup.ru).

REFERENCES

1. *Garini Y., Young I.T., McNamara G.* // Cytometry Part A. 2006. V. 69A. No. 10. P. 735.
2. *Deng L., Mao Z., Li X. et al.* // ISPRS. 2018. V. 69A. P. 124.
3. *Baier M.J., McDonald A.J., Clements K.A. et al.* // Proc. Com. Inst. 2021. V. 38. No. 3. P. 4433.
4. *Yu X., Sun Y., Fang A. et al.* // Proc. 2nd ICSAI (Shanghai, 2014). P. 871.
5. *Machikhin A.S., Khokhlov D.D., Batshev V.I., Pozhar V.E.* // Bull. Russ. Acad. Sci. Phys. 2018. V. 82. No. 11. P. 1403.
6. *Clancy N.T., Jones G., Maier-Hein L. et al.* // Med. Image Anal. 2020. V. 63. Art. No. 101699.
7. *Henriksen M.B., Garrett J.L., Prentice E.F. et al.* // Proc. 10th WHISPERS (Amsterdam, 2019). Art. No. 8921350.
8. *Minarík R., Langhammer J., Hanus J.* // Remote Sens. 2019. V. 11. No. 20. Art. No. 2428.
9. *Machikhin A.S., Batshev V.I., Kryukov A.V.* Method of simultaneous registration of multispectral images. Russian Federation patent No. 2800054, cl. G01J 5/08, G01J 3/02. 2023.
10. *Batshev V.I., Machikhin A.S., Krioukov A.V., Zolotukhina A.A.* // J. Opt. Tech. 2024. V. 90. No. 11. P. 706.
11. *Cao H., Gu X., Wei X. et al.* // Remote Sens. 2021. V. 12. No. 24. Art. No. 4012.
12. *Wu Y., Jiang S., Xu Z. et al.* // Front. Optoelectron. 2015. V. 8. No. 3. P. 319.
13. *Pu R.* Hyperspectral remote sensing: Fundamentals and practices. CRC Press, 2017. 466 p.
14. *Zolotukhina A., Machikhin A., Guryleva A. et al.* // Remote Sens. 2024. V. 16. Art. No. 1073.
15. *Croft H., Chen J.M., Luo X. et al.* // Glob. Chang. Biol. 2017. V. 23. No. 9. P. 3524.

FIGURE CAPTIONS

Figure 1. Illustration of registration of spectral images of an object by a multispectral camera based on optical aperture separation.

Figure 2. Multispectral camera data correction algorithm.

Figure 3. Spectral reflectance of individual regions of the color target measured by the spectrophotometer (solid line) and calculated from the multispectral camera data after correction (dashed line).

Figure 4. Illustration of the spectral images of the multispectral camera and the spatial distribution of chlorophyll concentration calculated from them.

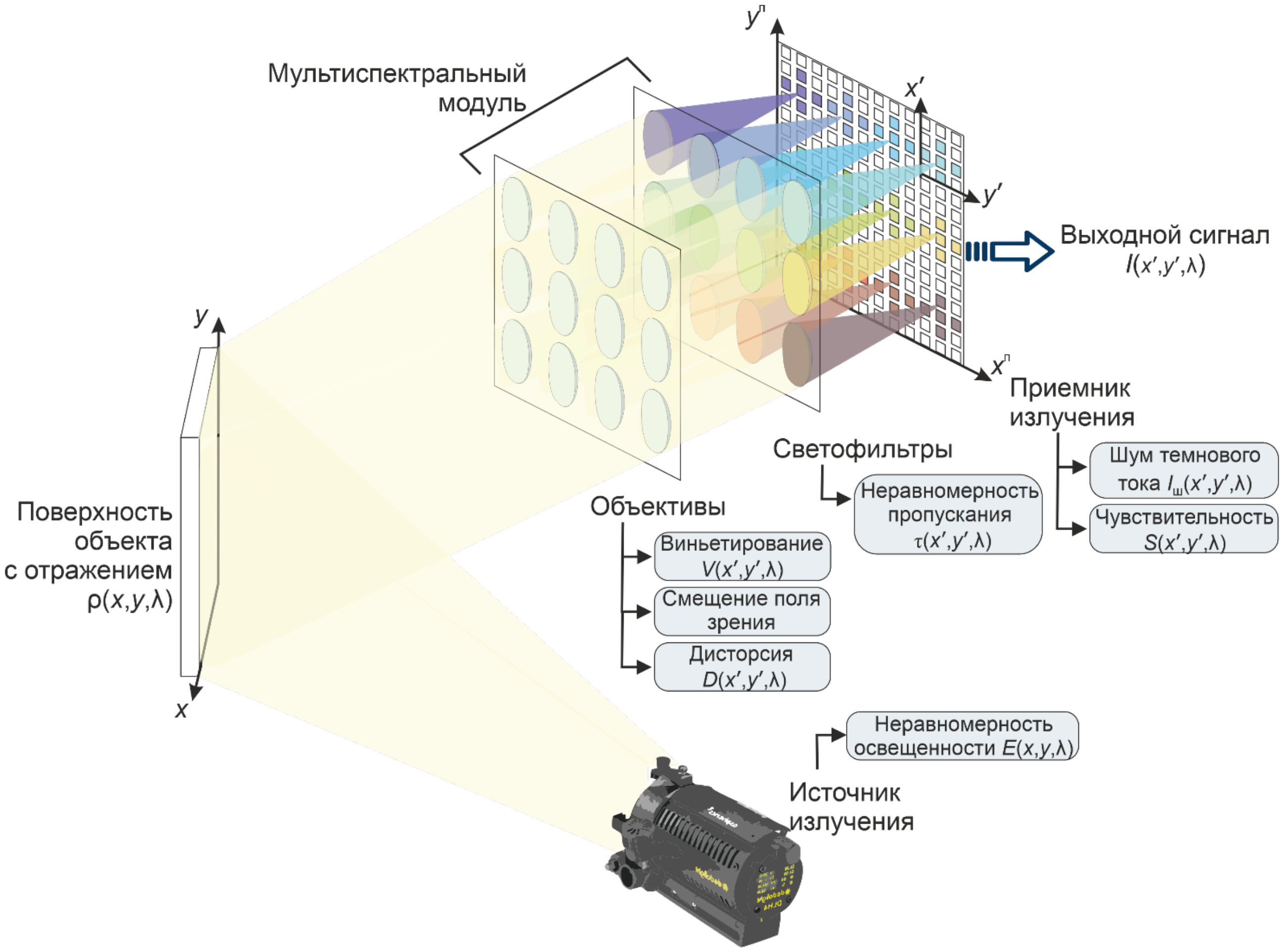
Мультиспектральный модуль
Выходной сигнал I(x′,y′,λ)
Приемник излучения
Шум темнового тока Iш(x′,y′,λ)
Чувствительность S(x′,y′,λ)
Светофильтры
Неравномерность пропускания τ(x′,y′,λ)
Объективы
Виньетирование V(x′,y′,λ)
Смещение поля зрения
Дисторсия D(x′,y′,λ)
Поверхность объекта с отражением ρ(x,y,λ)
Неравномерность освещенности E(x,y,λ)
Источник излучения

Fig. 1.

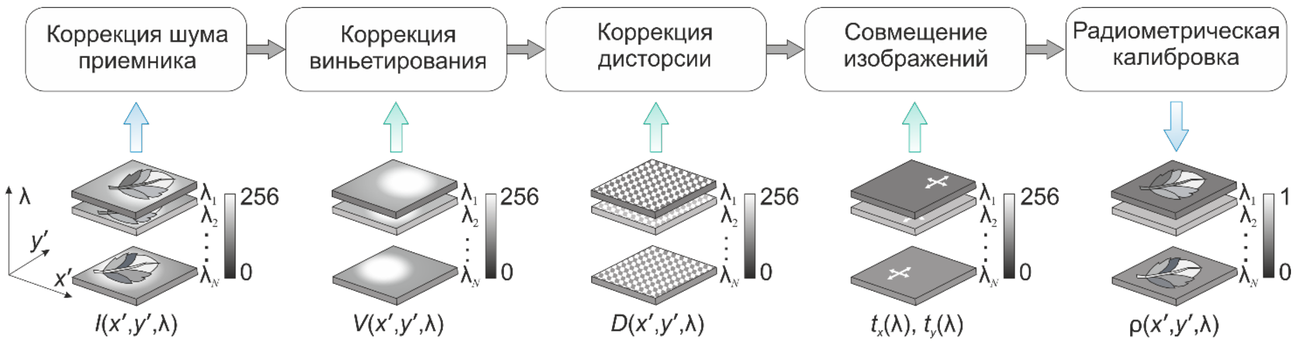
Коррекция шума приемника
Коррекция виньетирования
Коррекция дисторсии
Совмещение изображений
Радиометрическая калибровка
I(x′,y′,λ)
V(x′,y′,λ)
D(x′,y′,λ)
tx(λ), ty(λ)
ρ(x′,y′,λ)
256
0
1

Fig. 2.

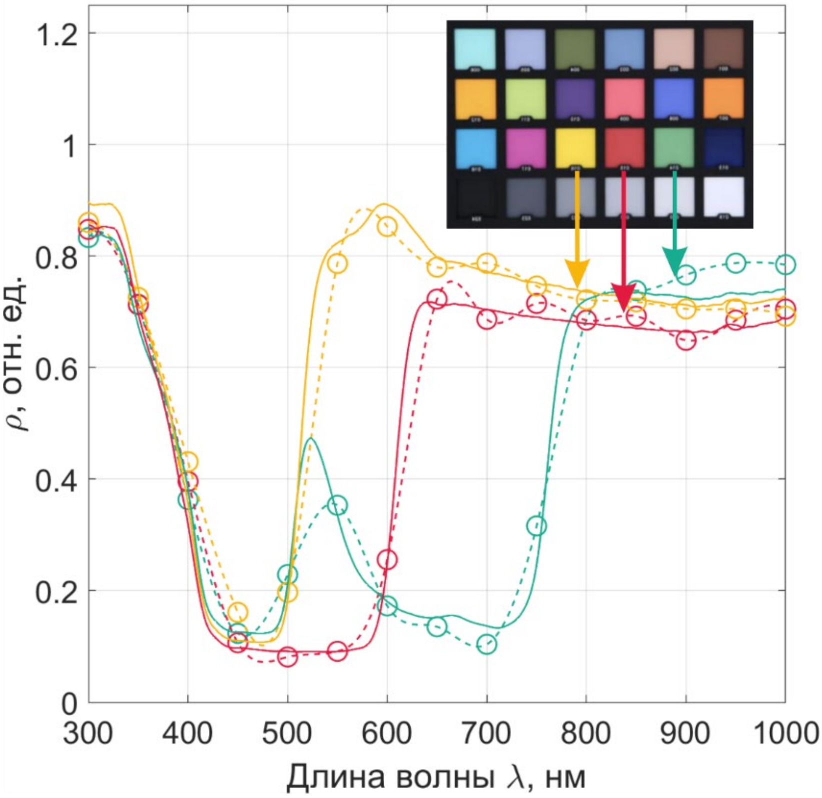

1.2
1
0.8
0.6
0.4
0.2
0
ρ, отн. ед.
300
400
500
600
700
800
900
1000
Длина волны λ, нм

Fig. 3.

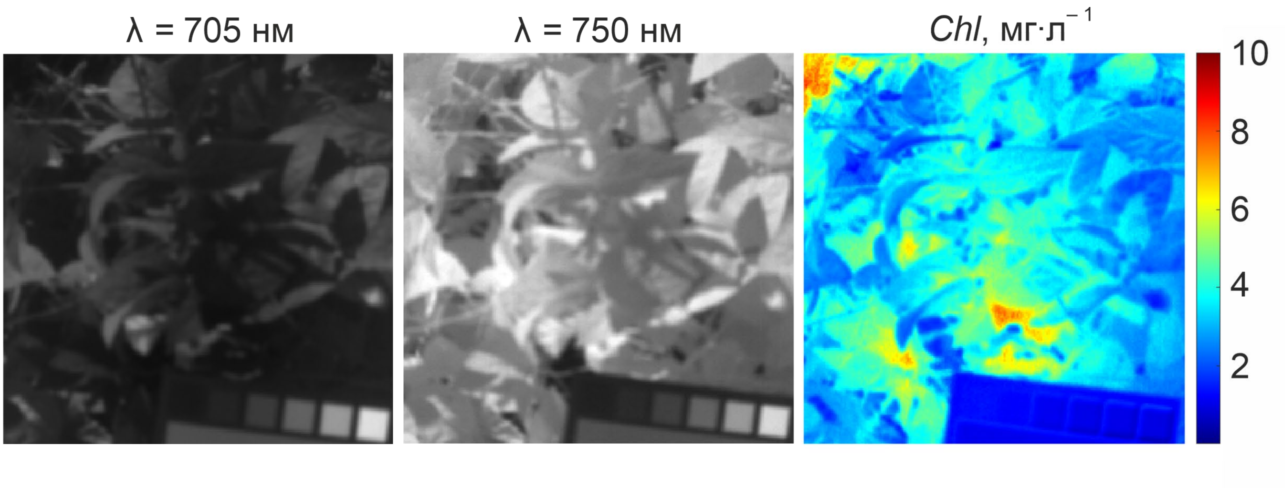

λ = 705 нм
λ = 750 нм
Chl, мг·л⁻¹
10
8
6
4
2

Fig. 4.